Virology 535 (2019) 122–129

Contents lists available at ScienceDirect

Virology

journal homepage: www.elsevier.com/locate/virology

Seneca Valley virus 2C and 3C inhibit type I interferon production by inducing the degradation of RIG-I

Wei Wen[a,b], Mengge Yin[a,b], Huawei Zhang[a,b], Tingting Liu[a,b], Huanchun Chen[a,b], Ping Qian[a,b], Junjie Hu[c], Xiangmin Li[a,b,*]

[a] State Key Laboratory of Agriculture Microbiology, Huazhong Agricultural University, Wuhan, 430070, PR China
[b] Division of Animal Infectious Diseases, College of Veterinary Medicine, Huazhong Agricultural University, Wuhan, 430070, China
[c] Hubei Colorectal Cancer Clinical Research Center, Hubei Cancer Hospital, Wuhan, 430071, China

ARTICLE INFO

Keywords:
Seneca valley virus
Degradation
2C
3C
RIG-I

ABSTRACT

Seneca Valley virus (SVV) is a member of the Picornaviridae family, which has been used to treat neuroendocrine cancer. The innate immune system plays an important role in SVV infection. However, few studies have elucidated the relationship between SVV infection and the host's antiviral response. In this study, SVV replication could induce the degradation of RIG-I in HEK-293T, SW620 and SK6 cells. And overexpressing retinoic acid-inducible gene I (RIG-I) could significantly inhibit SVV propagation. The viral protein 2C and 3C were essential for the degradation of RIG-I. Furthermore, 2C and 3C significantly reduced Sev or RIG-I-induced IFN-β production. Mechanistically, 2C and 3C induced RIG-I degradation through the caspase signaling pathway. Taken together, we demonstrate the antiviral role of RIG-I against SVV and the mechanism by which SVV 2C and 3C weaken the host innate immune system.

1. Introduction

Seneca Valley virus (SVV) belongs to the genus *Senecavirus* in the family *Picornaviridae*. SVV was originally isolated in Gaithersburg, Maryland, as a contaminant in adenovirus cultivation named SVV-001. The whole genome of SVV contains a single-stranded and positive-sense RNA containing about 7300 nt (Hales et al., 2008). Since vesicular disease caused by SVV was reported in Canada in 2007, a growing number of cases have been reported worldwide, severely threatening the swine industry (Leme et al., 2017; Pasma et al., 2008; Segales et al., 2017; Zhu et al., 2017). Despite its harm to the swine industry, SVV exhibits a selectively oncolytic property on neuroendocrine cancer, which has been found to be safe and effective in early-phase clinical trials (Burke, 2016; Liu et al., 2013; Poirier et al., 2013; Rudin et al., 2011).

The innate immune response is the host's first line of defense against viral invasion (Akira et al., 2006; Ishii et al., 2008). Pathogen-associated molecular patterns (PAMP) are recognized by pathogen recognition receptors (PRRs) during a viral infection, and subsequently trigger the production of type I interferon (IFN–I), which is capable of binding to IFN receptors and then inducing abundant IFN-stimulated genes (ISGs) (Sadler and Williams, 2008; Schoggins and Rice, 2011). Viral RNA can be recognized by Toll-like receptors (TLRs), which are located on the cell surface or cytoplasmic sensors such as retinoic acid-inducible gene I (RIG-I) and melanoma differentiation-associated gene 5 (MDA5) (Akira, 2009; Roers et al., 2016; Takeuchi and Akira, 2010). Once RIG-I is activated by viral RNA, the cascade recruitment domain (CARD) of RIG-I interacts with that of mitochondrial antiviral-signaling protein (MAVS) and then activates TANK-binding kinase 1 (TBK-1) and inhibitor of nuclear factor kappa-B kinase (IKK), which leads to the activation of interferon regulatory factor 3 (IRF3) and nuclear factor-B (NF-κB) (Loo and Gale, 2011; Servant et al., 2002). Subsequentely, the phosphorylation of IRF3 leads to its dimerization and nuclear localization and induces the expression of type I IFN (Sadler and Williams, 2008). Besides being a sensor, RIG-I can also function as effectors directly in antiviral immunity (Ahmad and Hur, 2015).

To prompt virus infection and replication efficiently, numerous viruses have evolved various strategies to antagonize innate immune signaling cascades (Schulz and Mossman, 2016). As RIG-I plays an important role in the innate immune response, several viruses can degrade or cleave RIG-I to attenuate antiviral immunity. For example, enteroviruses (EVs) suppress the antiviral response through cleaving various adaptor molecules (Lei et al., 2016). Foot-and-mouth disease virus (FMDV) degrades RIG-I using viral proteins including L, 3C, and

* Corresponding author. Division of Animal Infectious Diseases, College of Veterinary Medicine, Huazhong Agricultural University, 1 Shi-zi-shan Street, Wuhan, 430070, China.
E-mail address: lixiangmin@mail.hzau.edu.cn (X. Li).

https://doi.org/10.1016/j.virol.2019.06.017
Received 24 June 2019; Accepted 27 June 2019
Available online 28 June 2019

2B to inhibit the production the IFN-β (Zhu et al., 2016). West Nile Virus (WNV) non-structural protein NS1 and US11 protein of herpes simplex virus 1 (HSV-1) are identified as antiviral antagonists through the degradation of RIG-I and MDA5 or interference with the interaction between RIG-I and MAVS (Xing et al., 2012; Zhang et al., 2017). LMP1 of Epstein–Barr virus (EBV) degrades RIG-I through proteasome pathway to attenuate the host innate immune response (Xu et al., 2018). During poliovirus and encephalomyocarditis virus (ECMV) infection, RIG is cleaved and viral 3C protein is responsible for the cleavage (Barral et al., 2009).

Previous studies showed that SVV 3C cleaved adaptor proteins MAVS, TRIF and TANK and targeted IRF3 and IRF7 for degradation depending on its protease activity. Thus, the host innate immunity is damaged and the virus can replicate in host cells effectively (Qian et al., 2017; Xue et al., 2018). Nevertheless, other mechanisms where SVV viral proteins or RNA interacts with host cells to evade the host immune response remain to be fully elucidated. In this study, we determined that SVV can degrade RIG-I in comparison with that in uninfected cells. At the same time, overexpression of RIG-I could significantly decrease SVV propagation. The viral 2C and 3C were responsible for the degradation of RIG-I through the caspase signaling pathway and blocking the transcription of ISG56 and IFN-β.

2. Results

2.1. RIG-I is degraded in SVV-infected cells

RIG-I plays an important role in host innate immunity (Matsumiya and Stafforini, 2010). Previous studies showed that RIG-I is degraded or cleaved by viral proteins during FMDV and poliovirus infection (Barral et al., 2009; Zhu et al., 2016). The role of RIG-I in SVV-infected cells remains unknown. To characterize the state of RIG-I in SVV-infected cells, 293T cells were infected with SVV at a multiplicity of infection (MOI) of 1. Interestingly, the mRNA level of RIG-I hardly changed as the infected time increased, which was different from that in FMDV infected cells (Zhu et al., 2016) (Fig. 1A). We also measured the protein abundance of RIG-I at different infected time points. The protein level of RIG-I was gradually reduced in SVV-infected cells, which was inconsistent with the level of its mRNA. The amounts of RIG-I began to decrease at 6 hpi, and at 14 hpi, the band of RIG-I in 293T cells could not be detected through Western blot analysis (Fig. 1B). Consistent with this, RIG-I was also reduced in SW620 and SK6 cells infected with SVV (Fig. 1C and D).

2.2. Ectopic expression of RIG-I inhibits SVV replication

Previous studies revealed that RIG-I can function as dual receptors and effectors in antiviral immunity (Ahmad and Hur, 2015). To determine whether RIG-I has a suppressive effect in SVV infection, increasing amount of RIG-I was transiently overexpressed in 293T cells and the cells were infected with SVV (MOI of 0.1) at 24 hpt. The supernatant and cells were collected at 10 hpi to determine viral replication condition. Fig. 2A shows that the protein level of SVV structural protein VP1 was significantly downregulated in the presence of RIG-I with a dose-dependent effect. Moreover, relative mRNA levels of SVV were determined to demonstrate the antiviral effect of RIG-I against SVV (Fig. 2B). In addition, the viral titers measured in BHK-21 cells also showed the antiviral role of RIG-I to SVV (Fig. 2C).

2.3. SVV 2C and 3C induce the degradation of RIG-I

SVV infection was capable of degrading RIG-I. To determine which protein was essential for the reduction of RIG-I, RIG-I-Flag was co-transfected with various HA-tagged or GST-tagged viral proteins. The cells were collected to analyze protein expression at 24 hpt. As shown in Fig. 3A, SVV 2C and 3C significantly reduced the protein abundance of RIG-I in comparison with the control. To further investigate the impact of 2C and 3C on RIG-I expression, dose-dependent manner experiments were conducted. HEK-293T cells were co-transfected with an increasing dose of HA-2C or HA-3C and equal amounts of RIG-I-Flag for 24 h. As shown in Fig. 3B, the exogenous abundance of RIG-I was significantly reduced by 2C and 3C in a dose-dependent manner. In addition, we also determined the effects of 2C and 3C on endogenous RIG-I protein expression. HEK-293T cells were transfected with increasing amounts of HA-2C or HA-3C for 16 h and then stimulated with Sev for 12 h (Zhang et al., 2017). Consistent with exogenous RIG-I, endogenous RIG-I was also degraded by 2C and 3C in a dose-dependent manner. To investigate whether the reduction of RIG-I is attributed to the decrease of its mRNA by 2C and 3C, the mRNA level of RIG-I was determined with quantitative PCR. No significant reduction in the RIG-I mRNA level was observed (Fig. 3D). These results suggest that 2C and 3C protein target the translational or post-translational phase of RIG-I, resulting in its degradation.

2.4. SVV 2C and 3C inhibit RIG-I mediated IFN-β production

In accordance with the result of 2C and 3C on reduction of RIG-I, a luciferase reporter assay was performed to determine whether 2C and 3C participate in the suppression of Sev-induced IFN-β expression. As expected, we found 2C and 3C significantly show distant inhibitory level in Sev-induced IFN-β promotor activity (Fig. 4A). HEK-293T cells were co-transfected with HA-2C, HA-3C or empty vector and RIG-I-Flag. At 24 hpt, the cells were collected for Western blotting to analyze the phosphorylation level of IRF3 and the mRNA levels of IFN-β and ISG56. As shown in Figs. 4B, 2C and 3C significantly decreased the phosphorylation of IRF3 induced by RIG-I. Furthermore, 2C showed stronger inhibition on the phosphorylation of IRF3 than 3C induced by RIG-I. As expected, RIG-I-induced mRNA level of IFN-β and ISG56 were obviously reduced in the HEK-293T cells co-transfected with HA-2C or HA-3C (Fig. 4C). Collectively, these results suggest that SVV 2C and 3C block the phosphorylation of IRF3 and then reduce the expression of IFN-β and ISG56 through degrading RIG-I.

2.5. SVV 3C, not 2C, interacts with RIG-I

To determine whether 2C and 3C are capable of interacting with RIG-I, SK6 cells were co-transfected with HA-2C or HA-3C and RIG-I-Flag or empty vector for 24 h. The cell lysates were immunoprecipitated with anti-HA antibody. As shown in Fig. 5A, HA-3C could precipitate RIG-I-Flag, but not HA-2C. In addition, reverse immunoprecipitation was also conducted with anti-Flag antibody. Consistent with forward immunoprecipitated experiments, RIG-I-Flag could precipitate with HA-3C rather than HA-2C (Fig. 5B). Altogether, these results further suggested that SVV 2C can not interact with RIG-I. However, we observed a physical interaction between RIG-I and SVV 3C, which may provide the basic conditions for it to degrade RIG-I.

2.6. SVV 2C and 3C induce the degradation of RIG-I through the caspase pathway

Previous studies showed that RIG-I can be cleaved in picornaviruses-infected cells (Barral et al., 2009). To examine whether 2C and 3C could cleave RIG-I, HA-2C, HA-3C or empty vector was co-transfected with RIG-I-Flag in HEK-293T cells for 24 h. However, we did not find any specifically cleaved bands by Western blot analysis (Fig. 6A). To examine whether the caspase, proteasome or lysosome-dependent pathway participate in SVV 2C- and 3C-induced degradation of RIG-I, the caspase inhibitor Z-VAD-FMK, the lysosome inhibitor NH_4Cl and the proteasome inhibitor MG132 were used. Firstly, the cytotoxicity of all used inhibitors to HEK-293T cells was investigated with MTS assays. All inhibitors showed no detectable cytotoxicity in HEK-293T cells (Fig. 6B). Subsequently, HA-2C, HA-3C or empty vector was co-

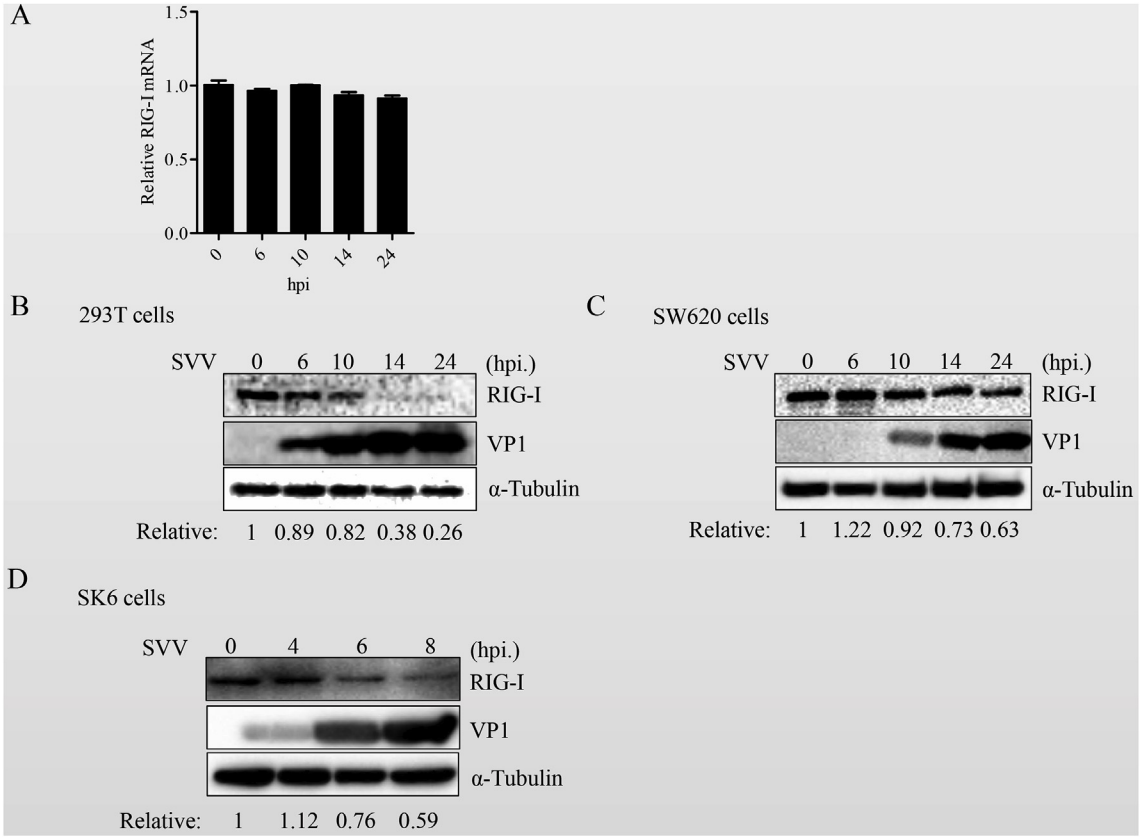

Fig. 1. SVV infection reduces the abundance of protein level of RIG-I. (A) 293T cells were infected with SVV at the indicated time points (0, 6, 10, 14, and 24 h). RIG-I mRNA level was analyzed by RT-qPCR, and housekeeping gene β-actin was used as the control. (B, C, D) 293T, SW620 or SK6 cells (2×10^5 cells in each well) were seeded in a 6-well plate. After 24 h, the monolayers were infected with SVV at an MOI of 1. The abundance of endogenous RIG-I, SVV VP1 protein, and α-Tubulin as an internal. Control were determined by Western blot analysis.

transfected with RIG-I-Flag. At 16 hpt, the HEK-293T cells were maintained in the presence of the inhibitors for 10 h and DMSO was used as a control eliminating its influence. As shown in Figs. 6C, 2C and 3C showed similar phenomenon, and the protein abundance of RIG-I was restored in the presence of Z-VAD-FMK. However, NH4Cl and MG132 had no influence on RIG-I rescue. SVV 3C contains a conserved catalytic box with histidine (His) and cysteine (Cys) residues. We further detected the impact of its protease activity on the degradation of RIG-I. Surprisingly, 3C mutants losing its protease activity could not degrade RIG-I (Fig. 6D). On account of caspase activity of 3C dependent on its protease activity(data not shown), we thought it futher indicated that 3C degraded RIG-I through caspase pathway. These findings demonstrate that SVV 2C and 3C target RIG-I for degradation through the caspase pathway.

3. Discussion

RLR-mediated type I IFN production is the host's first line of defense against invading viruses (Kato et al., 2006). To maintain effective infection, viruses have evolved several strategies to destroy the IFN cascade signaling (Takeuchi and Akira, 2009). During hepatitis B virus infection, RIG-I can disturb the interaction between P protein and viral pgRNA to inhibit viral replication (Sato et al., 2015). In addition, RIG-I binds to influenza A virus nucleocapsids of panhandles and restrains viral replication by destabilizing nucleocapsids (Weber et al., 2015). RIG-I acts as a pattern recognition receptor during picornavirus infection, which is important for host antiviral immune response (Buskiewicz et al., 2012; Feng et al., 2014). Viral protein 3C of several picornaviruses, such as poliovirus and EMCV, can target RIG-I for cleavage to impair its antiviral effects (Barral et al., 2009). WNV NS1 protein interacts with RIG-I and subsequently degrades it through proteasome pathway (Zhang et al., 2017). HCV NS4B induces the degradation of TRIF to inhibit TLR3 signaling pathway depending on caspase8 (Liang et al., 2018). In the present study, our results showed that SVV 2C and 3C target RIG-I for reduction through caspase-mediated protein degradation and then inhibited the phosphorylation of IRF3 and the production of IFN-β.

SVV, a member of the genus *Senecavirus*, was used as a potential treatment for small-cell lung cancer (Poirier et al., 2013; Wadhwa et al., 2007; Yu et al., 2011). The expression of IFN signaling genes played an important role in SVV replication. In addition to the cellular receptor ANTXR1, the downregulation of IFN signaling genes can be used as a classifier for SVV permissivity or nonpermissivity (Miles et al., 2017). SVV infection significantly suppressed the production of type I IFN through various strategies. SVV 3C, which contains a conserved catalytic box with His and Cys residues, could inhibit the production of IFN-β by targeting MAVS, TANK, and TRIF for cleavage (Qian et al., 2017). 3C also targeted IRF3 and IRF7 for degradation dependent on its protease activity (Xue et al., 2018).

Overexpression of RIG-I showed significant antiviral effects on SVV propagation. RIG-I could exhibit antiviral activity independent of IFN signaling (Rice et al., 2014), which may also work in SVV-infected cells. Previous studies showed that RIG-I was cleaved during various picornaviruses infection. In response to SVV infection, RIG-I was degraded in SVV-infected cells with 2C and 3C playing essential roles in this process (Fig. 3A to C). SVV 2C could not interact with RIG-I (Fig. 5A and B). Our data showed that 2C could cleave MAVS dependent on its induced apoptosis (data not shown). So we also detected whether RIG-I could be cleaved by 2C. Although SVV 3C could interact with RIG-I and possessed proteinase activity, no cleaved band of RIG-I could be

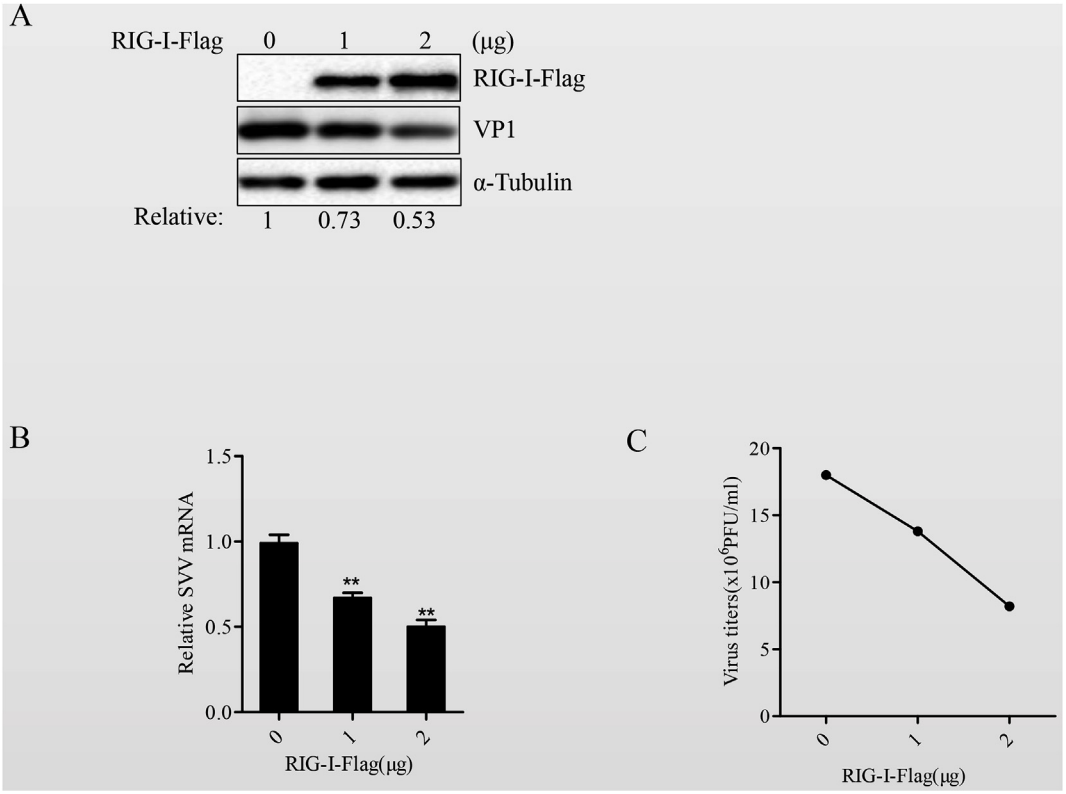

Fig. 2. Ectopic expression of RIG-I inhibits SVV propagation. 293T cells in 12-well plates were transfected with an increasing number of RIG-I expression plasmid, and the empty vector was used to ensure that cells in every plate obtained equal amount of total plasmids. At 24 hpt, the cells were infected with SVV at an MOI of 0.1 for 9 h. (A) Protein levels of SVV VP1 and exogenous RIG-I in 293T cells were determined by Western blot analysis. α-Tubulin served as an internal control. (B) Viral titers in culture supernatant of 293T cells were measured using plaque assay. (C) Relative quantification of intracellular SVV 5′UTR in 293T cells was determined by RT-qPCR.

observed in the presence of 3C (Fig. 6A). Interestingly, the caspase inhibitor (Z-VAD-FMK) significantly recovered the protein abundance of RIG-I, which indicated that the degradation was through the caspase-dependent pathway (Fig. 6C). Furthermore, the phosphorylation of IRF3 induced by RIG-I was reduced in the presence of 2C or 3C (Fig. 4B). In addition, SVV 2C and 3C also resulted in the reduced transcription of ISG56 and IFN-β stimulated by RIG-I (Fig. 4C). These data showed that SVV 2C and 3C can induce RIG-I degradation to block IRF3 activation and IFN-β production.

In conclusion, we determined the significant antiviral role of RIG-I during SVV infection. It was a novel mechanism that SVV 2C and 3C induced the degradation of RIG-I through the caspase pathway and inhibited RIG-I-mediated antiviral effect. SVV was sensitive to IFN-β and the enrichment of the gene set, INTERFERON_ALPHA_BETA_SIGNALING, played an important role in viral permissivity or non-permissivity (Miles et al., 2017). However, more studies are needed to analyze the relationship between SVV and the host's innate immune system.

4. Materials and methods

4.1. Cells and viruses

HEK-293T and BHK-21 cells were cultured in Dulbecco'smodified Eagle's medium (DMEM; Hyclone) containing 10% heat-inactivated fetal bovine serum (FBS; Gibico) in a 5% CO_2 incubator (37 °C). The SVV-HB strain (KX377924) was conserved in our laboratory (Qian et al., 2016). The viruses were propagated in BHK-21 cells and virus titers were also determined in BHK-21 cells using a PFU assay.

4.2. Plasmids and antibodies

The SVV individual proteins were amplified from SVV-HB cDNA. VP1, VP2, VP3, 2C, 3C, and 3D were cloned into vector pCAGGS-HA. L, 2B and 3A were cloned into plasmid pEBG-GST. RIG-I-Flag expressing vector was kindly provided by Meilin Jin (Huazhong Agricultural University). All constructs were identified by DNA sequencing.

The commericial antibodies used in the study included: an anti-Flag monoclonal antibody (Medical and Biological Laboratories, Japan), an anti-RIG-I polyclonal antibody (Abcam, Cambridge, MA, USA), an *anti*-pIRF3 monoclonal antibody (Cell Signaling Technology), an *anti*-IRF3 monoclonal antibody (Abcam, Cambridge, MA, USA), an anti-HA monoclonalantibody (Medical and Biological Laboratories, Japan), an *anti*-GAPDH monoclonal antibody (ProteinTech Group), an *anti*-α-Tubulin monoclonal antibody (ProteinTech Group), HRP-conjugated goat anti-rabbit IgG antibody (Medical and Biological Laboratories, Japan) and HRP-conjugated goat anti-mouse IgG antibody (Santa Cruz Biotechnology). A rabbit *anti*-VP1 polyclonal antibody was produced by our laboratory.

4.3. Immunoblotting and Co-immunoprecipitation

Cells transfected with different expressing vectors were collected and lysed for 30 min. Equal proteins were resolved by 12% sodium dodecylsulfate-polyacrylamide gels (SDS-PAGE) and transferred onto-polyvinylidene fluoride (PVDF) membrane (Roche, UK). The membrane was blocked with 5% skim milk in PBST for 2 h, and incubated with primary antibodies at room temperature for 2 h. After being washed with PBST for three times, it was incubated with secondary antibodies at room temperature for 1 h. Subsequently, All protein bands were virsualized using a Bio-Rad ChemiDoc XRS instrument and imaging

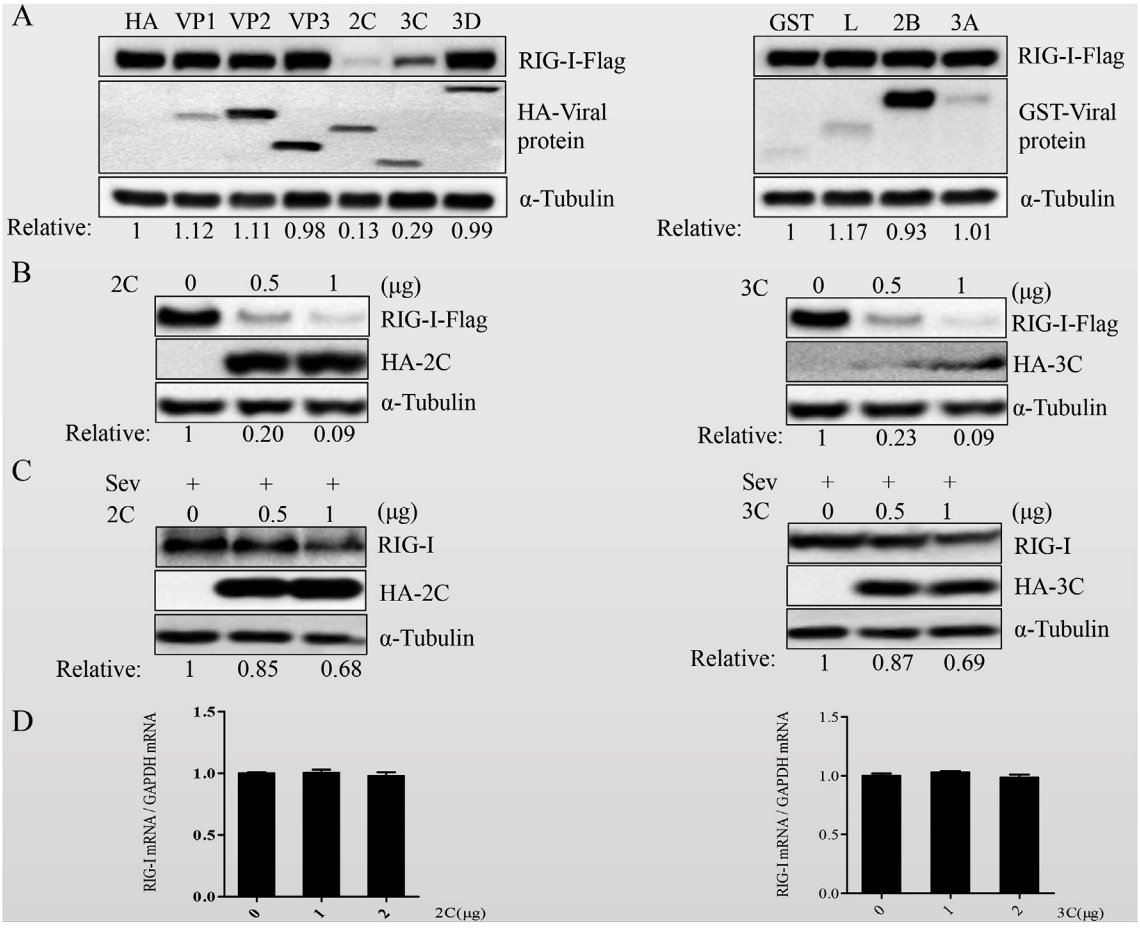

Fig. 3. SVV 2C and 3C induce the reduction of exogenous and endogenous RIG-I expression. (A) HEK-293T cells (1×10^5) were seeded in 24-well plates. After 24 h, RIG-I-Flag (0.5 μg) was co-transfected with HA- or GST-viral protein (0.5 μg). The cells were collected to analyze the expression of RIG-I and viral proteins by Western blot analysis at 24 hpt. (B) HEK-293T cells were seeded in 24-well plates. The monolayer cells were co-transfected with RIG-I-Flag (0.5 μg) and increasing amount of 2C or 3C (0, 0.5, 1 μg). The cells were collected for Western blot analysis at 24 hpt. (C) HEK-293T cells were seeded in 24-well plates, the monolayer cells were transfected with increasing amount of 2C or 3C (0, 0.5, 1 μg), and the cells were stimulated with Sev (HA titer, 32) at 16 hpt for 12 h. Then, exogenous RIG-I and viral protein were detected through Western blot analysis. (D) HEK-293T cells (1×10^6) were transfected with increasing number of HA-2C or HA-3C (0, 1, 2 μg) for 24 h, and the mRNA level of RIG-I was determined by RT-qPCR.

software. For the coimmunoprecipitation assay, HEK-293T cells in six-wells plates were co-transfected with a vector expressing Flag-RIG-I and an HA-2C/3C expression vector or an empty plasmid for 24 h. The cells were lysed with lysis buffer for 30 min on ice containing a protease inhibitor. The majority of cell lysates were then immunoprecipitated at 4 °C with mouse anti-Flag antibodies or anti-HA antibodies overnight. Subsequently, the immunoprecipitates were washed five times cold lysis buffer and were conducted an immunoblotting analysis.

4.4. Real-time PCR

TRIzol reagent (Invitrogen) was used to extract total RNAs following the manufacturer's protocol. Equal amount of RNA (1.0 μg) was conducted to synthesize cDNAs using HiScript II 1st Strand cDNA Synthesis Kit (Vazyme). The mRNA level of respective target gene was determined with qPCR using SYBR green real-time PCR master mix. The mRNA level of housekeeping gene β-actin was used as an internal control and all reactions were conducted in triplicate with similar results. The q-PCR primers are listed in Table 1 in this study. Relative gene fold was determined with the comparative cycle threshold (CT) ($2^{-\Delta\Delta CT}$) method.

4.5. Chemical inhibitors assay

HEK293T cells cultured in 24-well plates were co-transfected with the empty plasmid, HA-2C or HA-3C and Flag-RIG-I. After 16 h post transfection, the cells maintained with DMEM containing 10% FBS in the absence or presence of DMSO, the caspase inhibitor Z-VAD-FMK (Beyotime Biotechnology), proteasomal inhibitor MG-132 (Sigma-Aldrich) and lysosomal inhibitor NH_4Cl (Beyotime Biotechnology) for 10 h. Subsequently, the cells were collected and analyzed by western blotting.

4.6. MTS assay

The cytotoxicity of NH4Cl, MG132 and Z-VAD-FMK to 293T cells were determined with an MTS assay as described previously (Zhu et al., 2016). The experiments were repeated three times.

4.7. Statistical analysis

All experiments were conducted at least three times. The results were shown as values ± SE. Two-tailed Student's t-test was used to analyze the statistical significance. Statistical values of $^*P < 0.05$ was considered significant, and $^{**}P < 0.01$ was considered highly significant.

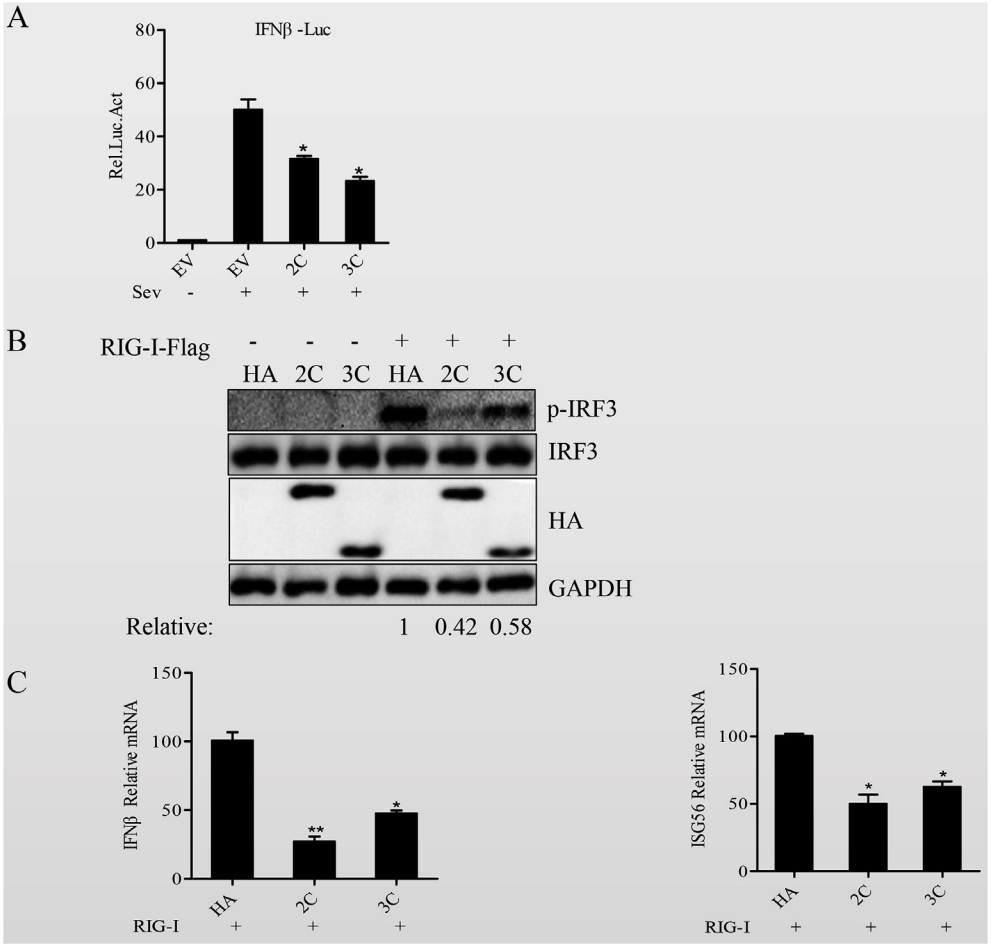

Fig. 4. SVV 2C and 3C block RIG-mediated IFN-β production. (A) HEK-293T cells were seeded in 24-well plates. Cells were cotransfected with a reporter plasmid encoding IFN-β-Luc plus pTK-Renilla and vector HA-2C or HA-3C. At 24 hpt, the cells were stimulated with Sev for 12 h. Then the firefly and Renilla luciferase activities were measured using a dual-luciferase reporter assay system. (B) HEK-293T cells were seeded in 12-well plates. After 24 h, HA-2C, HA-3C (1 μg), or vector was co-transfected with RIG-I-Flag (0.5 μg) for 24 h. The majority of cells were collected for immunoblotting analysis of IRF3 and phosphorylation of IRF3. (C) The expression of IFN-β and ISG56 mRNA was determined by RT-qPCR assay in another part of HEK-293T cells.

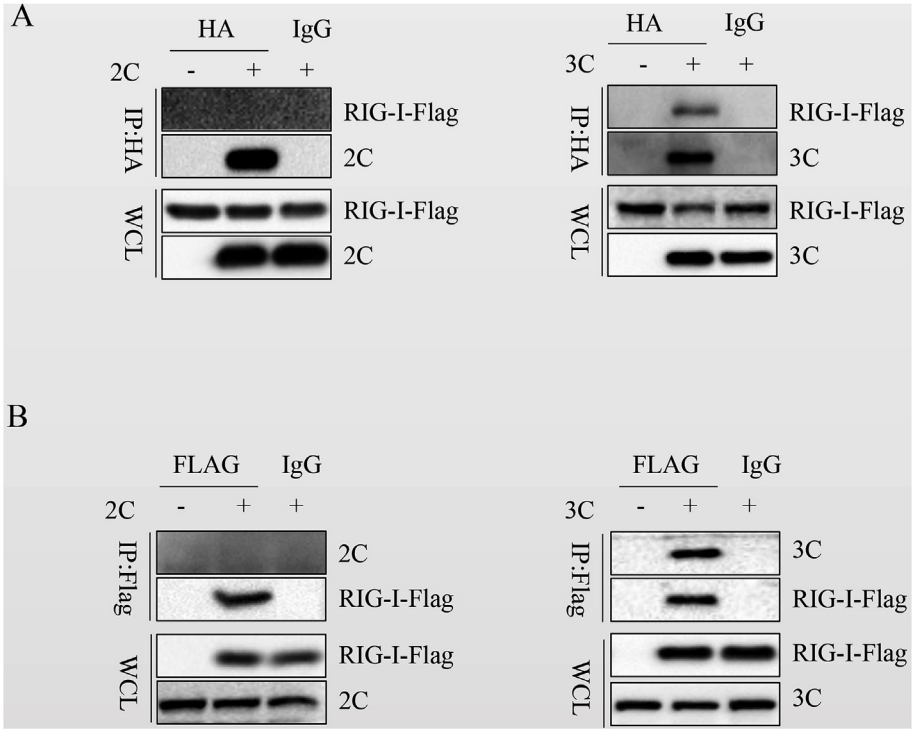

Fig. 5. SVV 3C, not 2C, interacts with RIG-I. (A) SK6 cells in 6-well plates were co-transfected with vector, 2C, or 3C (2 μg) and RIG-I-Flag (2 μg) for 24 h. The cell lysates were subjected to immunoprecipitation with rabbit anti-HA antibody, and the input and IP samples were analyzed by immunoblotting using mouse anti-Flag and rabbit anti-HA antibodies. (B) Similar transfection and immunoprecipitation experiments were conducted to verify the interaction.

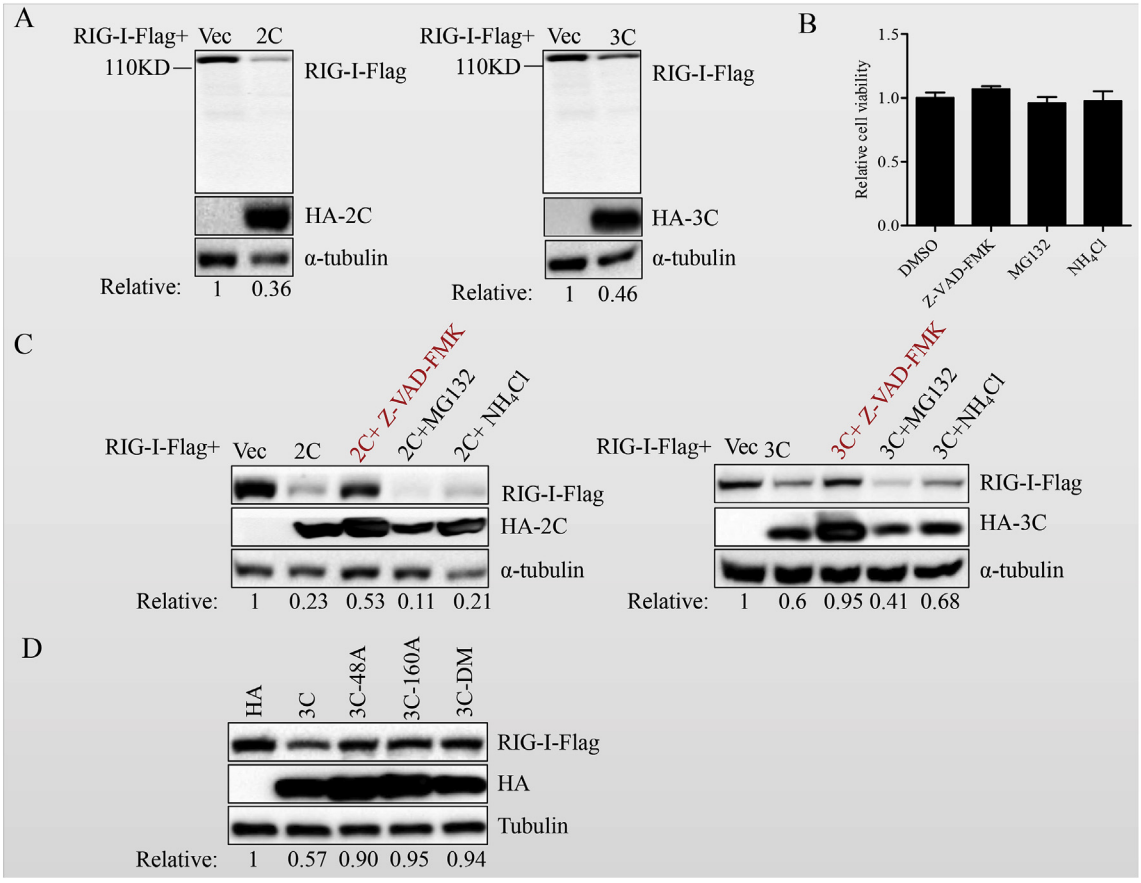

Fig. 6. SVV 2C and 3C induce the degradation of RIG-I through the caspase pathway. (A) HEK-293T cells (12-well plates) were co-transfected with 1 μg RIG-I-Flag and 1 μg vector, HA-2C, or HA-3C for 24 h. Then, the cells were collected for Western blot analysis. (B) HEK-293T cells were seeded in 96-well plates. When the confluence of cells reached 90%, the cells were maintained in the presence of DMSO, the proteasome inhibitor MG132, the caspase inhibitor Z-VAD-FMK, and the lysosome inhibitor NH_4Cl for 10 h. The cytotoxicity of the drugs on HEK-293T cells were evaluated using MTS assays. (C) HEK-293T cells in 24-well plates were co-transfected with 0.5 μg RIG-I and empty vector, HA-2C, or HA-3C. At 16 hpt, the cells were in the presence of DMSO, MG132, Z-VAD-FMK, and NH_4Cl for 10 h. (D) the monolayer cells in 24-well plate were co-transfected with RIG-I-Flag and vector, HA-3C or HA-3C-mutant-expressing plasmid. At 24 hpt, the cells were collected for western blotting.

Table 1
The primers used in the study.

Primers	Sequence(5′ to 3′)
RIG-I-F	CCAGGGATCCCAGCAATGAG
RIG-I-R	AAGCGTCCACAAGTGCTCTG
SVV-F	AACCGGCTGTGTTTGCTAGAG
SVV-R	GAACTCGCAGACCACACCAA
2C–F	GAATTCATGGGACCCATGGACAAAGTCAAAGAC
2C-R	CTCGAGCTACTGTAGAACTAGAGTCTGCATATTTCG
3C–F	GAATTCATGCAGCCCAACGTGGACATGGGCTTTG
3C-R	CTCGAGCTATTGCATTGTAGCCAGAGGTTCACC
ISG56-F	TCTGCCTATCGCCTGGATGG
ISG56-R	GCTTCAGGGCAAGGAGACC
IFN-β-F	TTGTTGAGAACCTCCTGGCT
IFN-β-R	TGACTATGGTCCAGGCACAG
β-actin	TGGACTTCGAGCAAGAGATGG
β-actin	GGAAGGAAGGCTGGAAGAGTG

Conflicts of interest

We declare that we have no financial and personal relationships with other people or organizations that can inappropriately influence our work.

Acknowledgements

This work was supported by National Program on Key Research Projects of China Grants 2018YFD0500204; the National Natural Science Foundation of China Grants 31772749, 31572495, 31772713; Fundamental Research Funds for the Central Universities Grant 2662017PY108.

References

Ahmad, S., Hur, S., 2015. Helicases in antiviral immunity: dual properties as sensors and effectors. Trends Biochem. Sci. 40, 576–585.
Akira, S., 2009. Pathogen recognition by innate immunity and its signaling. Proc. Jpn. Acad. B Phys. Biol. Sci. 85, 143–156.
Akira, S., Uematsu, S., Takeuchi, O., 2006. Pathogen recognition and innate immunity. Cell 124, 783–801.
Barral, P.M., Sarkar, D., Fisher, P.B., Racaniello, V.R., 2009. RIG-I is cleaved during picornavirus infection. Virology 391, 171–176.
Burke, M.J., 2016. Oncolytic Seneca Valley Virus: past perspectives and future directions. Oncolytic Virotherapy 5, 81–89.
Buskiewicz, I.A., Koenig, A., Huber, S.A., Budd, R.C., 2012. Caspase-8 and FLIP regulate RIG-I/MDA5-induced innate immune host responses to picornaviruses. Future Virol. 7, 1221–1236.
Feng, Q., Langereis, M.A., Olagnier, D., Chiang, C., van de Winkel, R., van Essen, P., Zoll, J., Hiscott, J., van Kuppeveld, F.J., 2014. Coxsackievirus cloverleaf RNA containing a 5' triphosphate triggers an antiviral response via RIG-I activation. PLoS One 9, e95927.
Hales, L.M., Knowles, N.J., Reddy, P.S., Xu, L., Hay, C., Hallenbeck, P.L., 2008. Complete genome sequence analysis of Seneca Valley virus-001, a novel oncolytic picornavirus. J. Gen. Virol. 89, 1265–1275.
Ishii, K.J., Koyama, S., Nakagawa, A., Coban, C., Akira, S., 2008. Host innate immune

receptors and beyond: making sense of microbial infections. Cell Host Microbe 3, 352–363.
Kato, H., Takeuchi, O., Sato, S., Yoneyama, M., Yamamoto, M., Matsui, K., Uematsu, S., Jung, A., Kawai, T., Ishii, K.J., Yamaguchi, O., Otsu, K., Tsujimura, T., Koh, C.S., Reis e Sousa, C., Matsuura, Y., Fujita, T., Akira, S., 2006. Differential roles of MDA5 and RIG-I helicases in the recognition of RNA viruses. Nature 441, 101–105.
Lei, X., Xiao, X., Wang, J., 2016. Innate Immunity Evasion by Enteroviruses: Insights into Virus-Host Interaction. Viruses 8.
Leme, R.A., Alfieri, A.F., Alfieri, A.A., 2017. Update on Senecavirus Infection in Pigs. Viruses 9.
Liang, Y., Cao, X., Ding, Q., Zhao, Y., He, Z., Zhong, J., 2018. Hepatitis C virus NS4B induces the degradation of TRIF to inhibit TLR3-mediated interferon signaling pathway. PLoS Pathog. 14, e1007075.
Liu, Z., Zhao, X., Mao, H., Baxter, P.A., Huang, Y., Yu, L., Wadhwa, L., Su, J.M., Adesina, A., Perlaky, L., Hurwitz, M., Idamakanti, N., Police, S.R., Hallenbeck, P.L., Hurwitz, R.L., Lau, C.C., Chintagumpala, M., Blaney, S.M., Li, X.N., 2013. Intravenous injection of oncolytic picornavirus SVV-001 prolongs animal survival in a panel of primary tumor-based orthotopic xenograft mouse models of pediatric glioma. Neuro Oncol. 15, 1173–1185.
Loo, Y.M., Gale Jr., M., 2011. Immune signaling by RIG-I-like receptors. Immunity 34, 680–692.
Matsumiya, T., Stafforini, D.M., 2010. Function and regulation of retinoic acid-inducible gene-I. Crit. Rev. Immunol. 30, 489–513.
Miles, L.A., Burga, L.N., Gardner, E.E., Bostina, M., Poirier, J.T., Rudin, C.M., 2017. Anthrax toxin receptor 1 is the cellular receptor for Seneca Valley virus. J. Clin. Investig. 127, 2957–2967.
Pasma, T., Davidson, S., Shaw, S.L., 2008. Idiopathic vesicular disease in swine in Manitoba. Can. Vet. J.= La revue veterinaire canadienne 49, 84–85.
Poirier, J.T., Dobromilskaya, I., Moriarty, W.F., Peacock, C.D., Hann, C.L., Rudin, C.M., 2013. Selective tropism of Seneca Valley virus for variant subtype small cell lung cancer. J. Natl. Cancer Inst. 105, 1059–1065.
Qian, S., Fan, W., Qian, P., Chen, H., Li, X., 2016. Isolation and full-genome sequencing of Seneca Valley virus in piglets from China, 2016. Virol. J. 13, 173.
Qian, S., Fan, W., Liu, T., Wu, M., Zhang, H., Cui, X., Zhou, Y., Hu, J., Wei, S., Chen, H., Li, X., Qian, P., 2017. Seneca Valley virus suppresses host type I interferon production by targeting adaptor proteins MAVS, TRIF, and TANK for cleavage. J. Virol. 91.
Rice, G.I., Del Toro Duany, Y., Jenkinson, E.M., Forte, G.M., Anderson, B.H., Ariaudo, G., Bader-Meunier, B., Baildam, E.M., Battini, R., Beresford, M.W., Casarano, M., Chouchane, M., Cimaz, R., Collins, A.E., Cordeiro, N.J., Dale, R.C., Davidson, J.E., De Waele, L., Desguerre, I., Faivre, L., Fazzi, E., Isidor, B., Lagae, L., Latchman, A.R., Lebon, P., Li, C., Livingston, J.H., Lourenco, C.M., Mancardi, M.M., Masurel-Paulet, A., McInnes, I.B., Menezes, M.P., Mignot, C., O'Sullivan, J., Orcesi, S., Picco, P.P., Riva, E., Robinson, R.A., Rodriguez, D., Salvatici, E., Scott, C., Szybowska, M., Tolmie, J.L., Vanderver, A., Vanhulle, C., Vieira, J.P., Webb, K., Whitney, R.N., Williams, S.G., Wolfe, L.A., Zuberi, S.M., Hur, S., Crow, Y.J., 2014. Gain-of-function mutations in IFIH1 cause a spectrum of human disease phenotypes associated with upregulated type I interferon signaling. Nat. Genet. 46, 503–509.
Roers, A., Hiller, B., Hornung, V., 2016. Recognition of endogenous nucleic acids by the innate immune system. Immunity 44, 739–754.
Rudin, C.M., Poirier, J.T., Senzer, N.N., Stephenson Jr., J., Loesch, D., Burroughs, K.D., Reddy, P.S., Hann, C.L., Hallenbeck, P.L., 2011. Phase I clinical study of Seneca Valley Virus (SVV-001), a replication-competent picornavirus, in advanced solid tumors with neuroendocrine features. Clin. Cancer Res. : Off. J. Am. Assoc. Cancer Res. 17, 888–895.
Sadler, A.J., Williams, B.R., 2008. Interferon-inducible antiviral effectors. Nat. Rev. Immunol. 8, 559–568.
Sato, S., Li, K., Kameyama, T., Hayashi, T., Ishida, Y., Murakami, S., Watanabe, T., Iijima, S., Sakurai, Y., Watashi, K., Tsutsumi, S., Sato, Y., Akita, H., Wakita, T., Rice, C.M., Harashima, H., Kohara, M., Tanaka, Y., Takaoka, A., 2015. The RNA sensor RIG-I dually functions as an innate sensor and direct antiviral factor for hepatitis B virus. Immunity 42, 123–132.
Schoggins, J.W., Rice, C.M., 2011. Interferon-stimulated genes and their antiviral effector functions. Curr. Opin. Virol. 1, 519–525.
Schulz, K.S., Mossman, K.L., 2016. Viral evasion strategies in type I IFN signaling - a summary of recent developments. Front. Immunol. 7, 498.
Segales, J., Barcellos, D., Alfieri, A., Burrough, E., Marthaler, D., 2017. Senecavirus A. Vet. Pathol. 54, 11–21.
Servant, M.J., Grandvaux, N., Hiscott, J., 2002. Multiple signaling pathways leading to the activation of interferon regulatory factor 3. Biochem. Pharmacol. 64, 985–992.
Takeuchi, O., Akira, S., 2009. Innate immunity to virus infection. Immunol. Rev. 227, 75–86.
Takeuchi, O., Akira, S., 2010. Pattern recognition receptors and inflammation. Cell 140, 805–820.
Wadhwa, L., Hurwitz, M.Y., Chevez-Barrios, P., Hurwitz, R.L., 2007. Treatment of invasive retinoblastoma in a murine model using an oncolytic picornavirus. Cancer Res. 67, 10653–10656.
Weber, M., Sediri, H., Felgenhauer, U., Binzen, I., Banfer, S., Jacob, R., Brunotte, L., Garcia-Sastre, A., Schmid-Burgk, J.L., Schmidt, T., Hornung, V., Kochs, G., Schwemmle, M., Klenk, H.D., Weber, F., 2015. Influenza virus adaptation PB2-627K modulates nucleocapsid inhibition by the pathogen sensor RIG-I. Cell Host Microbe 17, 309–319.
Xing, J., Wang, S., Lin, R., Mossman, K.L., Zheng, C., 2012. Herpes simplex virus 1 tegument protein US11 downmodulates the RLR signaling pathway via direct interaction with RIG-I and MDA-5. J. Virol. 86, 3528–3540.
Xu, C., Sun, L., Liu, W., Duan, Z., 2018. Latent membrane protein 1 of epstein-barr virus promotes RIG-I degradation mediated by proteasome pathway. Front. Immunol. 9, 1446.
Xue, Q., Liu, H., Zhu, Z., Yang, F., Ma, L., Cai, X., Xue, Q., Zheng, H., 2018. Seneca Valley Virus 3C(pro) abrogates the IRF3- and IRF7-mediated innate immune response by degrading IRF3 and IRF7. Virology 518, 1–7.
Yu, L., Baxter, P.A., Zhao, X., Liu, Z., Wadhwa, L., Zhang, Y., Su, J.M., Tan, X., Yang, J., Adesina, A., Perlaky, L., Hurwitz, M., Idamakanti, N., Police, S.R., Hallenbeck, P.L., Blaney, S.M., Chintagumpala, M., Hurwitz, R.L., Li, X.N., 2011. A single intravenous injection of oncolytic picornavirus SVV-001 eliminates medulloblastomas in primary tumor-based orthotopic xenograft mouse models. Neuro Oncol. 13, 14–27.
Zhang, H.L., Ye, H.Q., Liu, S.Q., Deng, C.L., Li, X.D., Shi, P.Y., Zhang, B., 2017. West nile virus NS1 antagonizes interferon beta production by targeting RIG-I and MDA5. J. Virol. 91.
Zhu, Z., Wang, G., Yang, F., Cao, W., Mao, R., Du, X., Zhang, X., Li, C., Li, D., Zhang, K., Shu, H., Liu, X., Zheng, H., 2016. Foot-and-Mouth disease virus viroporin 2B antagonizes RIG-I-mediated antiviral effects by inhibition of its protein expression. J. Virol. 90, 11106–11121.
Zhu, Z., Yang, F., Chen, P., Liu, H., Cao, W., Zhang, K., Liu, X., Zheng, H., 2017. Emergence of novel Seneca Valley virus strains in China. Transboundary Emerg. Dis. 64, 1024–1029 2017.